

# 1 **Effect of the morphology of hard segment domains in bio-based** 2 **polyurethanes on the filtration properties of nanostructured filters**

3 Simona Uhercova<sup>1\*</sup>, Dusan Kimmer<sup>1</sup>, Muhammad Yasir<sup>1</sup>, Lenka Lovecka<sup>1</sup>, Miroslava  
4 Kovarova<sup>1</sup>, Tomas Plachy<sup>1</sup> and Vladimir Sedlarik<sup>\*1</sup>

5 <sup>1</sup>*Centre of Polymer Systems, University Institute, Tomas Bata University in Zlín, Třída Tomáše Bati*  
6 *5678, 76001 Zlín, Czech Republic*

7 \*Corresponding authors: S.Uhercova ([s\\_dockalova@utb.cz](mailto:s_dockalova@utb.cz)), V.Sedlarik ([sedlarik@utb.cz](mailto:sedlarik@utb.cz))

## 8 **Abstract**

9 Renewable polymers have attracted significant attention in recent years as alternatives to  
10 fossil-based materials, driven by concerns about the depletion of such resources and the need  
11 for sustainable development. This study reports on the synthesis of polyurethanes from  
12 renewable biomass-derived diols, and their subsequent application in nanostructured air filters  
13 produced via electrospinning. Comparison is made of the properties of bio-based  
14 polyurethane samples that varied in the molecular weights of the inherent poly(1,3-  
15 propanediol) soft segments. Their physical-mechanical properties were analysed, along with  
16 the morphology and filtration performance of the nanostructures. It was found that the  
17 arrangement of the hard segments affected both phase temperature transitions (i.e. the glass  
18 transition and melting point) of the prepared polyurethanes. Positive effect hard segments  
19 domain arrangements and the best filtration properties were observed for a bio-polyether-  
20 based aromatic polyurethane prepared with a molar ratio of diisocyanate:polyether  
21 polyol:chain extender of 4.7:1:3.7 and a molar mass of used renewable polyol 1000 g/mol, a  
22 nanostructure boasting the largest pore size of those tested. Filter with pressure drop of 49 Pa  
23 only possessed a quality factor exceeding 0.045 Pa<sup>-1</sup>. The work confirms the fact that the  
24 effects of fiber diameter and pore size on the filtration properties of nanostructured air filters  
25 fabricated to eliminate ultra-fine particles cannot be judged separately.

26 **Keywords:** Biomass, synthesis of polyurethanes, electrospinning, nanofiber membrane, air  
27 filtration.

## 28 1. INTRODUCTION

29 The chemical industry is transitioning to renewable and sustainable plastics in response to  
30 economic and ecological concerns about the future usage of fossil raw materials [1]. This  
31 trend has been reflected in the adoption of polyurethane (PU), a form of plastic which can be  
32 varied to have wide-ranging properties and applications. Examples of the latter include types  
33 of glue and sealant, flexible and rigid foam, liquid paint and varnish, solutions employed in  
34 the manufacture of synthetic leather and thermoplastic elastomers (TPU) [2,3]. PU for  
35 filtration application is often chosen as a material composing a nanostructure due to its  
36 chemical stability good chemical properties (first of all glass transition temperature – Tg),  
37 excellent nanofiber forming characteristic [4,5].

38 One of the main reasons for using PUs is that the properties of PU can vary in a wide range,  
39 so it is possible to adjust them for many applications [6]. PU nanostructures have application  
40 in high-performance air filters, protective textiles, wound dressing materials, sensors and  
41 biomedical applications. PU can be mixed with other polymers and fillers e.g. carbon  
42 nanotubes [7,8].

43 Bio-based raw materials (e.g. 1,3-propanediol and 1,4-butanediol) have only been made  
44 commercially available at low cost with sufficient purity to synthesize PU for a short period  
45 of time [9]. Recent advances in bioprocessing [10–12] have also boosted the production of  
46 bio-based raw materials for the synthesis of PU, such as 1,4-butanediol (BD), succinic acid  
47 and adipic acid [10–13]. Great interest has been paid lately to PUs fabricated from bio-based  
48 materials since environmental resources are becoming ever more scarce [14–19]. Applying  
49 bio-based polyols in PU chemistry, therefore, affords the opportunity for sustainable and  
50 environmentally-friendly systems [20,21]. Bio polyols synthesized from bio-based  
51 1,3-propanediol have been used, for instance, in the production of PU reactive hot-melt  
52 adhesive [22]; the DuPont company also offers poly(1,3-propanediol) (PPD) as a 100%  
53 renewable polyol [23]. Polyols constitute a key raw material in the fabrication of PUs, and are  
54 primarily produced from fossil-fuels, namely petroleum, which has held back research on  
55 alternatives [24], although moves are afoot for a gradual shift from fossil-based to biomass-  
56 based polyols [25]. The latter can be synthesized from lignin [26], agricultural waste [27,28],  
57 vegetable oil [29–34] and other renewable resources. Elastomers formulated from bio-based  
58 PUs, wherein bio polyols constitute a raw material, are an example of a practical application  
59 that has garnered interest [35–39].

60 Thermoplastic polyurethane elastomers (TPU) are segmented polyadducts with a two-phase  
61 domain microstructure consisting of hard and soft segments [40–42]. The high modulus of  
62 TPU is attributable to hard block domains made from hard segments, which act as cross-  
63 linked, physically bonded crystalline centres dispersed in the soft segment of flexible polyol  
64 chains. The hard block domains, therefore, act as molecular reinforcing fillers. Another reason  
65 for researching the PPD diols comprised the fact that polyethers tend to be less compatible  
66 with 4,4'-methylene-diphenyl diisocyanate (MDI) than polyester diols, hence TPU derived  
67 from them shows a higher degree of phase separation. Increasing the length (molecular  
68 weight) of the soft segment diols would promote domain separation too [24].

69 Polyether TPU is usually formulated from poly(oxytetramethylene) diols  
70 (polytetrahydrofuran). It was synthesized herein from renewable polypropylene diols with an  
71 identical content of hard segments ( $w_{HS} = 60\%$  by mass). The given concentration was  
72 informed by a prior study, wherein high modulus TPU with a maximum tested volume of hard  
73 segments (the molar ratio was MDI:polymeric diol:BD and equalled 9:1:8) exerted a positive  
74 influence on the efficiency of nanofiber formation in an electrostatic field [43]. The hard  
75 segment domains consisted of aligned chains of urethane groups interlinked by hydrogen  
76 bonds in three dimensions. With respect to PU samples prepared from bio-based 1,3-  
77 propanediol (PU 500) at a molar ratio of 2.5:1:1.5, almost an entirely alternating arrangement  
78 of hard and soft segments was expected, resulting in a material with numerous, small, evenly  
79 dispersed hard segments in the soft segment portions.

80 The first commercial PU fiber was developed in Germany in the early 1940s [2]. It was made  
81 by reacting hexamethylene diisocyanate with a slight excess of 1,4-butanediol. Elastic fibers,  
82 commonly referred to as Spandex are the most notable concerning mass production, and  
83 constitute a generic term approved by the US Federal Trade Commission.

84 An area of study that has recently proven popular concerns the development of air filtration  
85 materials capable of removing pollutants, especially dangerous nano-sized ones (particles up  
86 to 1  $\mu\text{m}$  in size) [44–46]. Filters based on nanofibers with a low fiber diameters have become  
87 more effective at eliminating ultra-fine particles, retaining low pressure drop of the filter  
88 [45,47]. The filtration properties of nanostructured materials fabricated by electrospinning are  
89 generally superior to those of filters prepared from meltblown materials [48]. Besides PU  
90 [49–53], fossil-based polymers frequently applied in the production of nanofibers in an

91 electrostatic field include polyvinylidene fluoride (PVDF) [44,54], polyacrylonitrile (PAN)  
92 [55,56], polysulfone (PSU) [52,57], polyethersulfone (PESU) and polyamide (PA) [58,59].

93 The primary novelties of this work lie in i) synthesis of PU from renewable resources (bio-  
94 based diols) with addressing environmental and sustainability aspects, ii) finding optimal  
95 morphology of hard segments in tested PU which provides creation of bulky nanostructure  
96 with bigger pore sizes guaranteeing better air filtration performance with regard to the capture  
97 of ultra-fine particles in sizes from 20 nm to 400 nm in consequence of Brownian motion, iii)  
98 set up very efficient nanostructure via electrospinning for air filtration caused by arrangement  
99 of hard segments in bio-based PU. All of those novelties extend the desired level of filtration  
100 efficiency, pressure drop and thence quality factor.

## 101 **2. EXPERIMENTAL**

### 102 *2.1 Materials*

103 4,4'-methylene-diphenyl diisocyanate (MDI), bio-based polyether polyols (PPD 500, 1000,  
104 and 2000 g/mol), 1,4 butanediol (BD) and N, N-dimethylformamide (DMF) were purchased  
105 from Sigma-Aldrich (Germany). Sodium tetra-borate decahydrate (Borax) and citric acid were  
106 bought from PENTA (Czech Republic).

### 107 *2.2 Preparation of the polymer solutions*

108 PU samples were fabricated via a polyaddition reaction involving the diisocyanate, bio-based  
109 polyether diols (soft segment) and chain extender, by means of one-shot synthesis in DMF  
110 solvent; the content of hard segments (diisocyanates + chain extenders) was maintained at  
111 60% by mass. Prior to conducting such synthesis, the various PPD diols had been dried in a  
112 vacuum at 90°C for ca 30 minutes. The MDI and BD were then added, and the reaction  
113 proceeded at 90°C for 3 to 4 hours. DMF was supplemented stepwise once the viscosity of the  
114 PU solution had started to increase. The concentrations (*c*) were adjusted to 18%, 16% and  
115 15% by mass, respectively, corresponding to viscosities ( $\eta$ ) from 2100 to 2400 mPa s, suitable  
116 for the electrospinning process. Electrical conductivity  $\chi$  was increased to a value higher than  
117 200  $\mu\text{S}/\text{cm}$  by the addition of DMF solution (18.6% by mass) of Borax and citric acid at the  
118 ratio of 1:3 for the electrospinning process. The samples of PU solutions for the  
119 electrospinning process were prepared in molar ratios detailed jointly with resulting  
120 concentration, conductivity and viscosity in Table 1.

121 **Table 1.** Properties of the synthesized PU solutions and thermoplastic PU (TPU) dry extracts.

Material marking*	Molar ratio	After synthesis		After adjustment for the electrospinning process			Content of renewable material (% by mass)
		c <sub>s</sub> (% by mass)	η <sub>s</sub> (mPa s)	c <sub>ES</sub> (% by mass)	η <sub>ES</sub> (mPa s)	χ (μS/cm)	
PU 2000	9:1:8	20	13200	18	2400	207	54.7
PU 1000	4.7:1:3. 7	20	10640	16	2200	231	53.1
PU 500	2.5:1:1. 5	20	4790	15	2100	242	50.4

122 \* compared samples possessed the same content of hard segments, i.e. 60% by mass

### 123 2.3 Fabrication of nanofibers

124 Nanostructures with a width of 40 cm were produced in an electrostatic field from the PU  
 125 solutions on a SpinLine 40 electrospinning device (SPUR, Czech Republic), equipped with 32  
 126 fiber-forming nozzles arranged in two lines. The experimental conditions under which the PU  
 127 nanofibers were spun comprised the following: an applied electric voltage of 75 kV; the  
 128 distance between electrodes measured 20 cm; the polymer solution was dosed at 0.5 mL/min;  
 129 the substrate movement rate was 0.2 m/min; the temperature equalled 23±2°C; and the  
 130 relative humidity was 31%. The nanofibers were deposited on polyethylene terephthalate or  
 131 polypropylene nonwoven substrate, which lent mechanical support to the subsequent  
 132 nanostructured filters. All the nanostructures of various thicknesses and surface areas were  
 133 prepared under uniform electrospinning process conditions; thus, the parameters for  
 134 fabrication were not individually optimized for each solution.

### 135 2.4 Characterization of the synthesized PU and prepared nanostructures

#### 136 2.4.1 Fourier-transform infrared spectroscopy

137 Fourier-transform infrared attenuated total reflectance (FTIR-ATR) was employed to  
 138 characterize the chemical composition of the prepared nanofibers (Nicolet iS5, Thermo Fisher  
 139 Scientific, Waltham, USA); this occurred at the wavenumber range of 4000–400 cm<sup>-1</sup>, 64  
 140 scans per spectrum and resolution of 4 cm<sup>-1</sup>, with analysis in OMNIC software (Thermo  
 141 Fisher Scientific, Waltham, USA).

#### 142 2.4.2 Contact angle

143 The water contact angles (Θ<sub>w</sub>) of the samples were gauged with adherence to EN 15802.  
 144 Measurement was performed at laboratory temperature on a Surface Energy Evaluation

145 System (Advex Instruments, Czech Republic), with evaluation of the data taking place in  
146 SeeSystem 7.0 software.

#### 147 *2.4.3 Differential Scanning Calorimetry*

148 The thermal behavior of synthesized PU was determined by differential scanning calorimetry  
149 (DSC) on a DSC 1 STAR (Mettler Toledo, Switzerland) instrument. Measurements were  
150 recorded during such thermal analysis in an inert nitrogen atmosphere (50 mL/min) across a  
151 temperature range of 0 to 250°C. The rate for heating and cooling was set at 10°C/min.

#### 152 *2.4.4 Dynamic Mechanical Analysis*

153 The viscoelastic properties of the PU samples were evaluated by dynamic mechanical analysis  
154 (DMA; DMA 1; Mettler Toledo) under tension mode. The linear viscoelastic region (LVE)  
155 was determined initially by performing an amplitude sweep. A temperature sweep followed,  
156 applying a strain within a range of the LVE region across temperatures of –80 to 40°C, at a  
157 heating rate of 3°C/min and frequency of 1 Hz. Glass transition temperatures ( $T_g$ ) were  
158 obtained as peaks for viscous moduli ( $E''$ ), since this approach corresponds well with the  
159 other thermal analyses employed to determine  $T_g$ .

#### 160 *2.4.5 Tensile tests*

161 Tensile tests were conducted to determine values for tensile strength and Young's modulus on  
162 a Testometric universal machine (MT350-5CT); this happened in accordance with EN ISO  
163 527 at a single-strain rate of 500 mm/min and room temperature. The specimens had been  
164 conditioned at 25°C and 50% relative humidity for 72 hours before such testing took place.  
165 Each set of samples consisted of at least 5 specimens.

#### 166 *2.4.6 Scanning electron microscopy (SEM)*

167 A Phenom Pro scanning electron microscope was used to examine the morphology of the  
168 material. In order to avoid an electrostatic charge accumulating during morphological  
169 observations, the surfaces of samples were sputter-coated with Au/Pd prior to the test. SEM  
170 was used to image electrospun fibers to observe the surface morphology and any defects, such  
171 as a bead in the structure, that might be incorporated during electrospinning and to determine  
172 the desired diameter of nanofibers. The electron beam was operated at an accelerating voltage  
173 of 10kV. The mean diameter of fibers was measured via ImageJ version 1.52a software  
174 (National Institutes of Health and the Laboratory for Optical and Computational  
175 Instrumentation (LOCI, University of Wisconsin), Madison, Wisconsin (USA)).

#### 176 2.4.7 Determination of porometry

177 Characteristics relating to the pore sizes of the membranes were assessed on a flow porometer  
178 (SPUR, Czech Republic) in accordance with ASTM F316-03 (2011); Galpor (Porometer,  
179 Belgium) was employed as a wetting liquid. Dry and wet tests were conducted on three  
180 circular samples cut out from the given materials and mean values were obtained for them.  
181 The resulting porosity measurements encompassed the mean pore diameters of the  
182 nanostructures and the maximum pore diameters; pore size distributions were counted as well.

#### 183 2.4.8 Filtration efficiency

184 The filtration properties of samples were measured on a TSI 3160 fractional efficiency filter  
185 tester. The investigation took place at an aerosol NaCl flow rate of 30 L/min and a face  
186 velocity of 5.2 cm/s. The quality factor (quality filter,  $q_F$ ) constituted an important parameter  
187 with regard to filtration performance, and was calculated by the following equation:

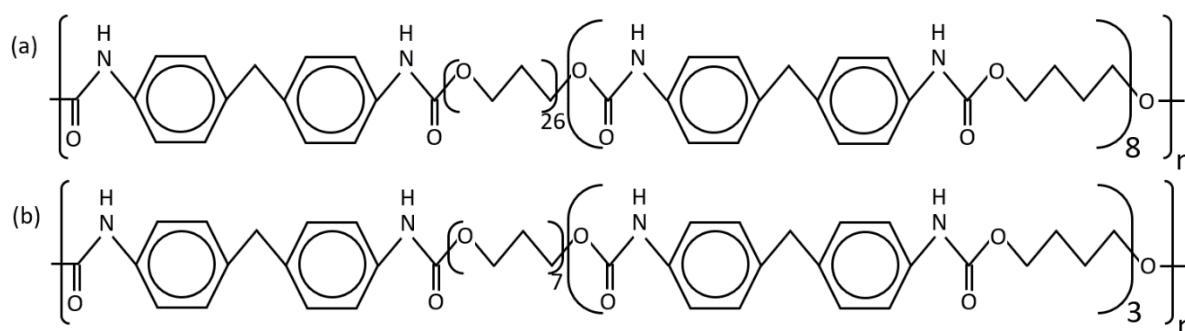
$$q_F = \frac{\ln(1/P)}{\Delta p} \quad (1)$$

188 where P stands for penetration ( $P = 1 - E$ ), E is efficiency and  $\Delta p$  is the pressure drop.

### 189 3. RESULTS AND DISCUSSION

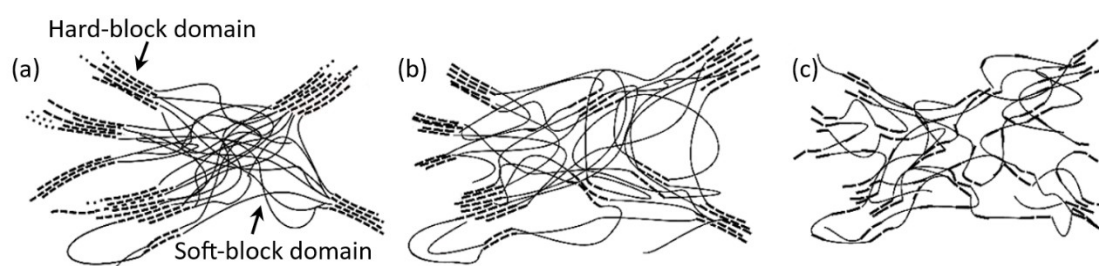
#### 190 3.1 Synthesis of PU solutions

191 “One-shot” way of PU synthesis was used for the preparation of PU solutions for  
192 the submicron fiber forming process in an electrostatic field. The process of polyaddition  
193 reaction with both bio polymeric diol and bio low molecular diol was very similar to reactions  
194 based on fossil diols with strictly difunctional monomers. Their purity from the viewpoint of  
195 functionality request was very high, content of used difunctional bio diols was higher than  
196 99%. Properties of prepared PU solutions after synthesis and after adjustment for fabrication  
197 in electrostatic are summarized in Table 1. Idealized chemical composition of synthesized  
198 PUs with the highest and lowest content of hard segments is represented in Figure 1.  
199 Synthesized polyurethanes differed in hard segment morphology and length of soft segments.



203 *3.2 Electrospinning process*

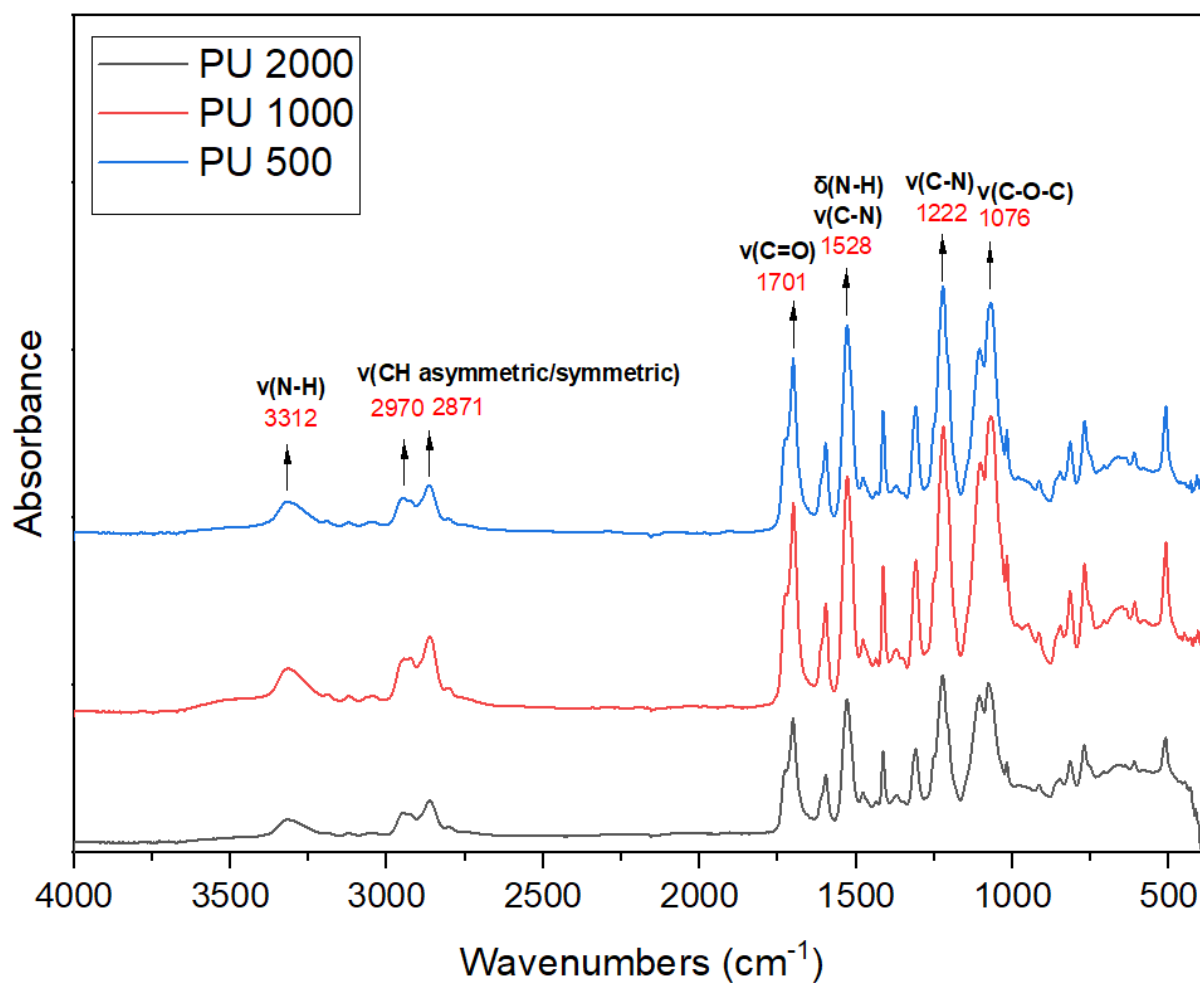
204 Three various nanostructures were created from synthesized PU solutions despite the fact that  
 205 all of them were fabricated under uniform electrospinning process conditions. Those differ  
 206 first of all in nanofiber diameters and pore sizes. We suppose that nanofibers with lower fiber  
 207 diameter will be more flexible and create a formation with smaller pore sizes, whereas  
 208 nanofibers with higher fiber diameter will be tougher, more flexible and a more reinforced  
 209 structure with larger pore sizes will arise. Brownian motion dominantly effects the filtration  
 210 efficiency in the area of ultrafine particle capture; consequently higher nanostructure with  
 211 larger pore sizes (bringing about lower pressure drop) can positively affect filtration  
 212 performance [60–62]. Figure 2 presents the idealised morphological arrangement of the hard  
 213 segments in the tested PU structures.



217 *3.3 Fourier transform infrared spectroscopy*

218 The chemical structures of the bio-based PU nanofibers were analysed from FTIR spectra. As  
 219 detailed in Figure 3, all the spectra show peaks typical for an aromatic PU derived from a  
 220 polyether diol. The vibration bands at 3312 and 1528  $\text{cm}^{-1}$  correspond to -NH stretching,  
 221 while the peaks in the region spanning 3000 to 2770  $\text{cm}^{-1}$  relate to -CH responses to  
 222 asymmetric and symmetric stretching vibrations. The wavenumbers at 1528 and 1222  $\text{cm}^{-1}$   
 223 are attributed to frequencies of the -CN group, whereas the band at 1076  $\text{cm}^{-1}$  pertains to

224 symmetric -C-O-C- stretching. Confirmation that the monomers had reacted fully and  
225 appropriate polymerization conditions had transpired is provided by a peak absent from the  
226 curves at ca 2270  $\text{cm}^{-1}$  that would otherwise represent free -NCO groups [60–62].



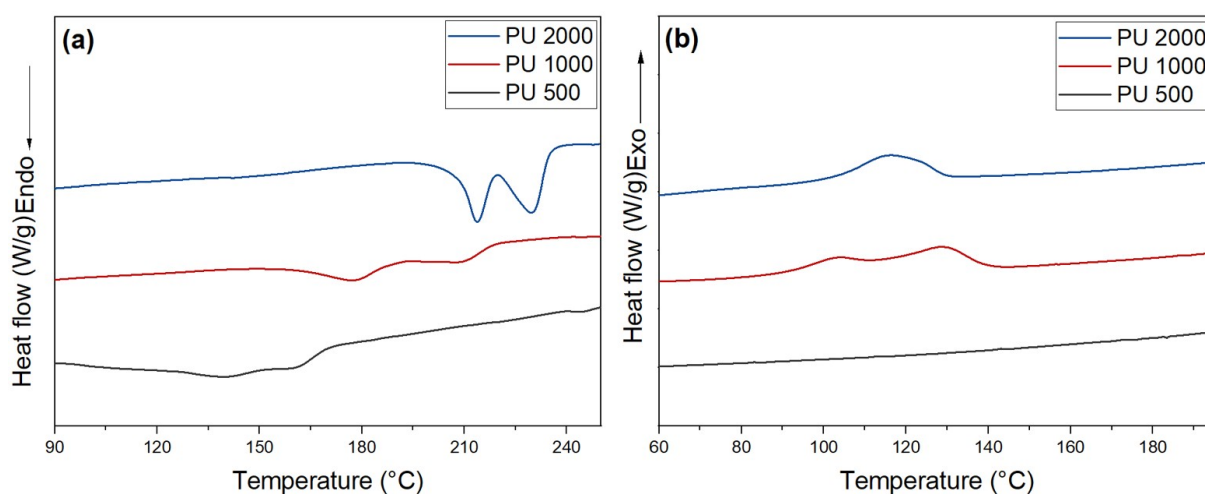
227

228

**Fig. 3.** FTIR spectra obtained in ATR mode for the tested PU materials.

### 229 3.4 Differential scanning calorimetry

230 Determining changes in the melting and crystallization temperatures permitted DCS  
231 investigation of the morphology of hard segment domains and variation in the lengths of the  
232 soft segments in the PPD-derived, bio-based PU. Incorporating soft segment polyols that  
233 varied in molecular weight in the specimens, while maintaining a constant, uniform weight  
234 fraction of hard segments, yielded synthesized PU materials with melting temperatures ( $T_m$ ) of  
235 between 141°C and 214°C, these outer values being recorded for PU 500 and PU 2000,  
236 respectively; PU 1000 had an intermediate melting temperature of approximately 178°C  
237 (Table 2). As illustrated in Figure 4a, this parameter rose in parallel with an increase in the  
238 molecular weight of the PPD applied, a phenomenon attributed to the arrangement of the hard  
239 segments (see Fig. 3). The broad endothermic peak observed for the PU 500 and 1000  
240 samples could be explained by the limited extent of structural order within the hard segment  
241 domains. In contrast, the PU 2000 sample exhibited a more pronounced and intense double  
242 peak, indicating a greater degree of arrangement [63]. This heightened regularity in structure  
243 is also evidenced in Figure 4b, where a crystallization peak appears at 116°C for the PU 2000  
244 specimen. The PU 1000 sample presents a double peak at 128°C, indicating a reduction in  
245 such regularity in comparison with PU 2000. The absence of an exothermic peak in the PU  
246 500 sample, however, suggests the existence of a highly disordered structure which would  
247 inhibit crystallization.



248

249

**Fig. 4.** DSC curves for the PU materials: (a) heating and (b) cooling.

### 250 3.5 Contact angles

251 The hydrophilicity of the synthesized nanostructured materials was gauged through recording  
252 contact angle measurements. The nanostructured PU materials tended to exhibit hydrophilic

253 properties, as indicated by the water contact angles observed below 60° (see Table 2). This  
 254 indicates that the molecular weights of the polyether diols did not influence the hydrophilicity  
 255 of the prepared PU samples.

### 256 3.6 Mechanical properties of the synthesized PU

#### 257 3.6.1 Tensile test

258 The state of hard segment aggregation is affected by the soft segments present. Polyether diols  
 259 tend to be less compatible with MDI than those in polyester, and TPU derived from them  
 260 shows a higher degree of phase separation, hence hard segment domains are usually larger  
 261 and more complex. Increasing the molecular weight of the given diol also favours domain  
 262 separation.

263 A tensile test was conducted to evaluate the stiffness of the materials. Every PU sample  
 264 contained the same concentration of hard segments, fixed at 60% by mass. Their elevated  
 265 hardness most likely arose from this uniformity in composition, made up of hard segments in  
 266 large, well-defined domains. The PU 2000 specimen, as anticipated, exhibited the greatest  
 267 stiffness, approximately 234 MPa. This was attributed to the superior arrangement of rigid  
 268 segments within its polymer matrix. Moreover, it had the highest tensile strength. The PU  
 269 1000 and 500 samples demonstrated similar values to each other for Young's modulus and  
 270 tensile strength, varying merely within standard deviation (Table 2); this finding was ascribed  
 271 to the inadequate organization of hard segments within their structures. Arrangements of hard  
 272 segments result to bulkier structure with larger pore sizes (PU 1000 – optimum structure from  
 273 the filtration performance point of view) or on the contrary concise, less bulky structures with  
 274 lower pore sizes (PU 2000 – large hard segments domains and PU 500 with spread hard  
 275 segments, unreinforced, easy deformable structure). The measurement of filtration efficiency  
 276 was done for NaCl particles in sizes 20 through 400 nm where Brownian motion dominantly  
 277 affect the mechanism of particle capture.

278 **Table 2.** Data on the physical-mechanical properties of the bio-based PU materials, obtained  
 279 by measurement of contact angles, tensile testing, DSC and DMA.

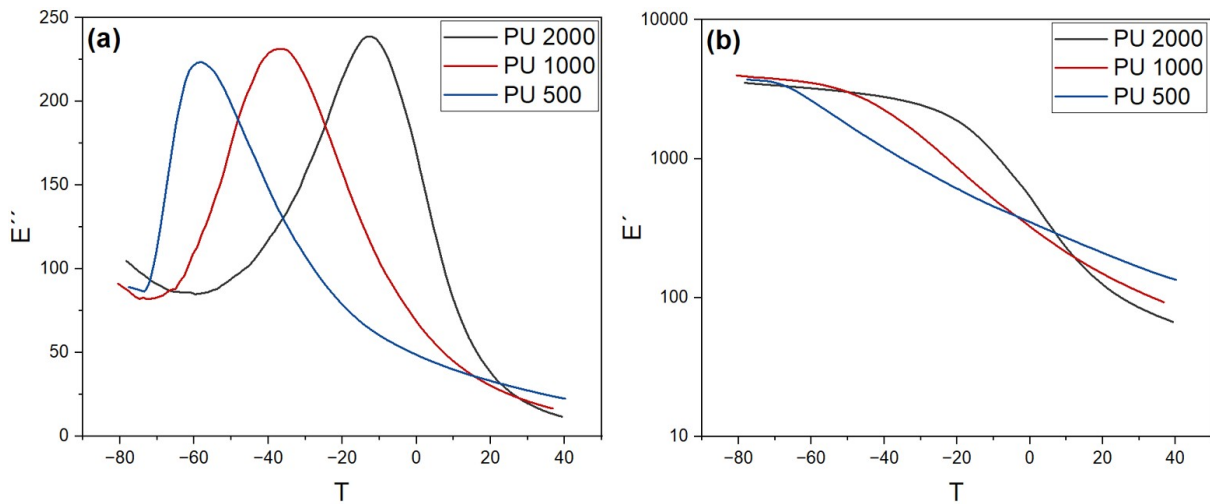
Material designation	Θ <sub>w</sub> (°)	Young's modulus (MPa)	Tensile strength (MPa)	Temperature of melting (°C)	Elastic modulus (MPa)	Glass transition temperature (°C)
PU 2000	51.0±4.6	234.0±19.9	28.5±4.7	214	3 520	-12.6
PU 1000	58.9±2.5	135.9±13.1	11.5±2.5	178	3 982	-35.7

PU 500	57.5±4.1	168.5±8.4	12.8±1.2	141	3 709	-58.2
--------	----------	-----------	----------	-----	-------	-------

280        *3.6.2 Dynamic mechanical analysis*

281 DMA confirmed the significant impact of precursor selection on the viscoelastic properties  
 282 of the PU samples. Applying polyether soft segments that differed in molecular weight  
 283 and the ratio of MDI:BD (although the mass content of hard segments was the same in each  
 284 sample) resulted in PU systems with values for  $T_g$  of -58.2°C, -35.7°C and -12.6°C, pertaining  
 285 to the PU 500, 1000 and 2000 specimens, respectively (see Fig. 4a). These observations  
 286 corresponded with the transition of polyether soft segments in the PU chains [64], since  
 287 an increase in molecular weight reduced the extent of free volume, thereby significantly  
 288 raising values for  $T_g$  [65].

289 Every sample was similar in terms of its elastic modulus ( $E'$  get about in the range from 3520  
 290 to 3982 mPa s) when in a glassy state (see Fig. 4b). Since the content of MDI and BD in each  
 291 was comparable, the elastic modulus in this region was primarily determined by strong  
 292 interactions of the isocyanate segments [63]. In the viscoelastic region, however, it was the  
 293 influence of the polyol soft segments that predominated and directly altered the associated  
 294 behaviour of the PU samples. Despite the PU 500 specimen exhibiting the lowest  $T_g$  and  
 295 slowest decrease in  $E'$  values, the values recorded for it at room temperature exceeded those  
 296 of every other PU sample. Notably, the softening process for the PU 2000 sample began at the  
 297 highest temperature as it possessed the highest  $T_g$ , although the high mobility of its long  
 298 polyol chains triggered a rapid drop in values for  $E'$ . It was concluded that the overall  
 299 viscoelastic properties of the samples were strongly influenced by two factors: i. the  
 300 arrangement of hard segments, and ii. the combination of their lengths of polyether soft  
 301 segments and MDI: BD ratios.



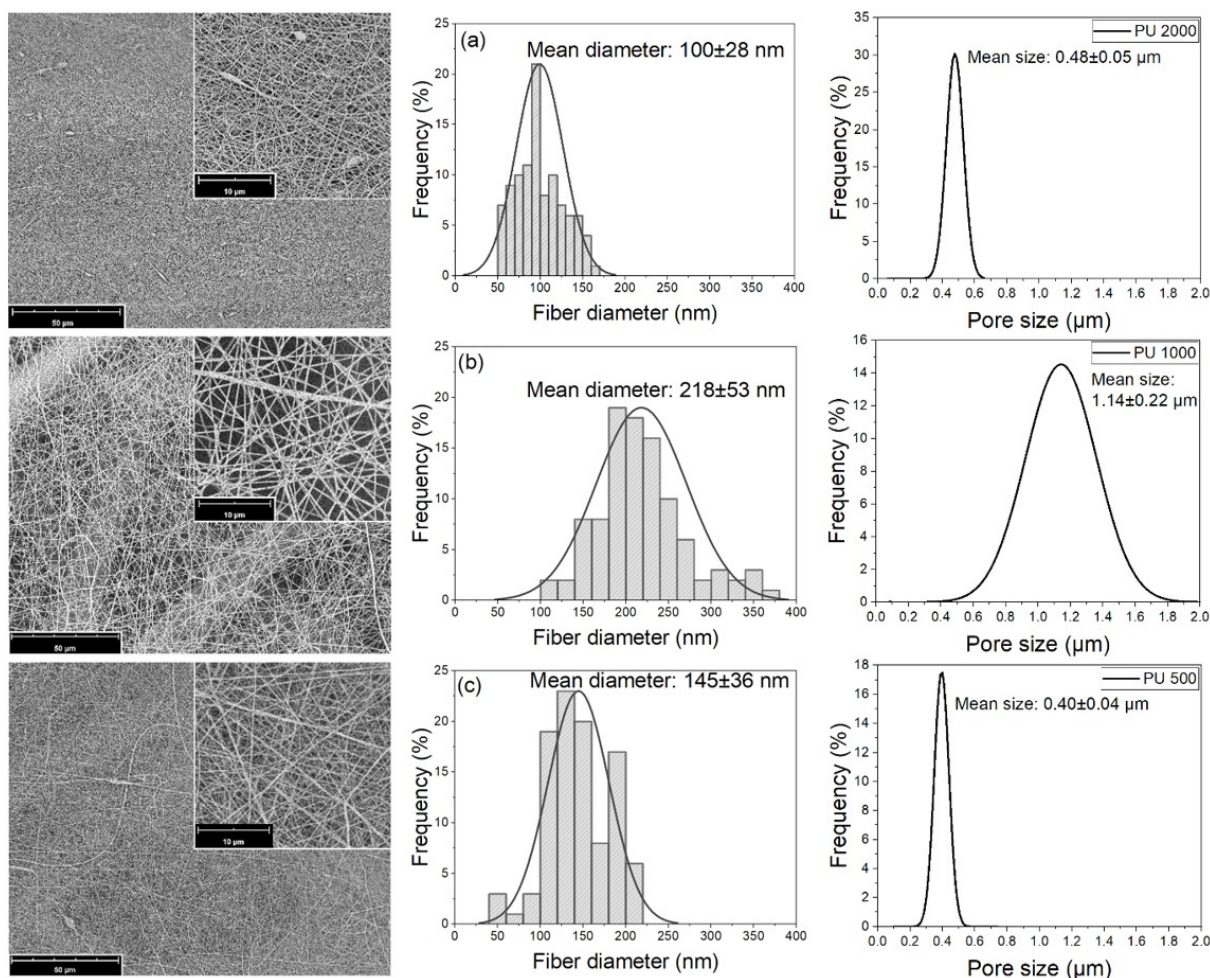
302

303 **Fig. 5.** DMA analysis of the prepared PUs: a) dependence of loss modulus on temperature and  
 304 b) semi-log dependence of elastic modulus on temperature.

305

### 3.6.3 Scanning electron microscopy

306 The morphology of the nanostructured layers was characterized by comparing SEM images  
 307 at 5000× magnification and measuring the diameters of nanofibers (see Fig. 6). The data  
 308 obtained on the distribution of values for all the tested nanostructures were processed  
 309 graphically. Despite the fact that the conditions for electrospinning and properties of the  
 310 treated solutions were almost identical, differences in nanostructures existed. For example,  
 311 the nanofibers of the PU 1000 sample were straight, thicker and more reinforced than  
 312 elsewhere and constituted a nanostructure possessing larger pore sizes with low pressure drop.  
 313 Nevertheless, the ultrafine particles exerting considerable Brownian movement are  
 314 intercepted very effectively.



315

316 **Fig. 6.** Surface morphologies of the electrospun PU filters and their respective nanofibers, in  
 317 addition to the pore diameter distributions of: a) PU 2000, b) PU 1000 and c) PU 500.

318 *3.6.4 Pore sizes*

319 The most critical aspects for the pore sizes of the nanostructures were thickness  
 320 of nanostructure, basic weight, as well as the diameters and flexibility of the given nanofibers.  
 321 These significantly affected certain parameters of the pores, as follows: i) average pore size  
 322 diameter, ii) maximum pore size diameter; and iii) distribution of pore diameters. Each  
 323 material was evaluated for its morphology and filtration performance. While PU 1000  
 324 possessed the lowest tensile strength and Young's modulus, its fiber diameter, average and  
 325 maximum pore sizes, and associated distribution exceeded those of PU 2000 and PU 500 (see  
 326 Tab. 3 and Fig. 6).

327 **Table 3.** Characterization of the nanostructures by SEM and porometry.

Material designation	Fiber diameter (nm)		Pore size (µm)	
	Mean	Min.-Max.	Mean	Maximum
PU 2000	100±28	52–167	0.48±0.05	0.62

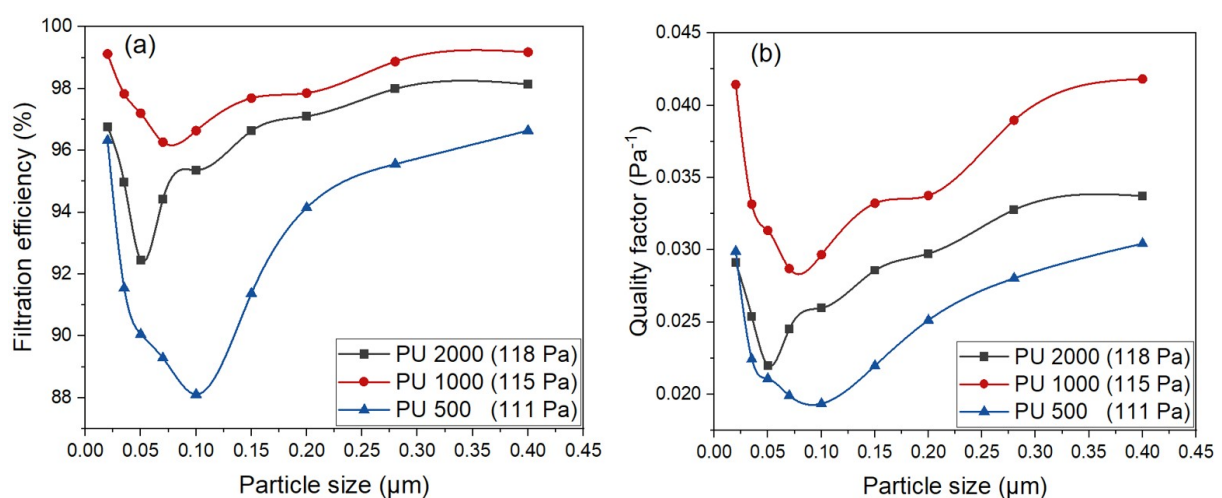
PU 1000	218±53	108–365	1.14±0.22	1.84
PU 500	145±36	59–211	0.40±0.04	0.54

328 For confirmation of the effect exerted by the arrangements of hard segment domains  
 329 on the pore sizes of the nanostructures and, consequently, filtration performance, values for  
 330 the diameters of the nanofibers should be very similar or even identical.

### 331 3.6.5 Filtration properties

332 Three filters made of PU nanostructures based on bio PPD with variable molar weights are  
 333 compared from the filtration efficiency and quality factors point of view. With growing  
 334 pressure drop, the filtration efficiency is increasing, while, in the case of recognition by means  
 335 of quality factors with a growing pressure drop of filters, the  $q_F$  is partially decreasing.

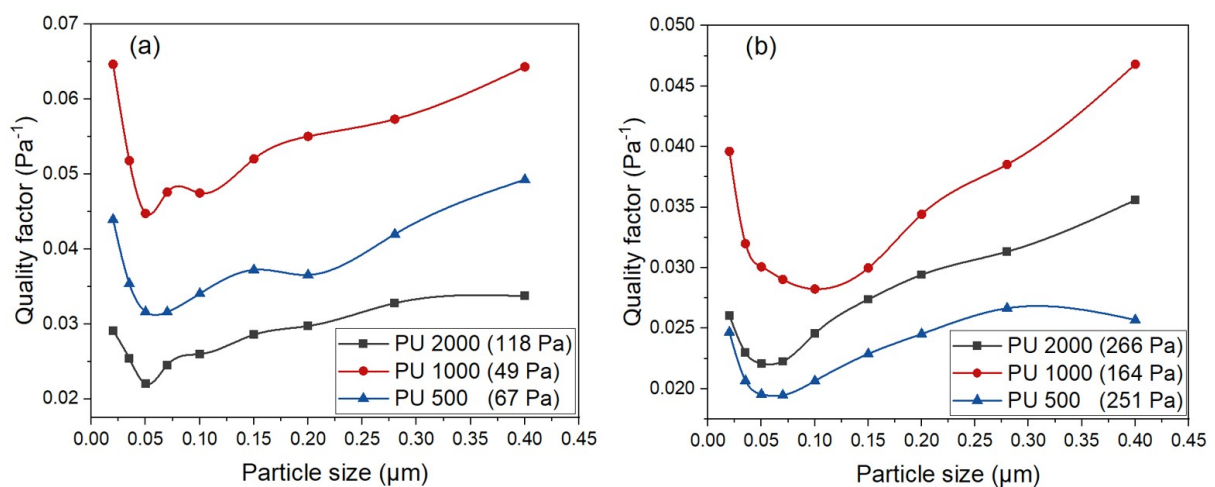
336 To evaluate the filtration efficiency of tested filtration materials, a comparison of filters  
 337 with the same values of pressure drops is necessary (Fig. 7a). The ones analysed had pressure  
 338 drops of 111 Pa to 118 Pa, with filtration efficiency rising in the sequence of PU 1000 >  
 339 PU 2000 > PU 500. The PU 2000 nanofibers measured ca 100 nm in diameter (hence were  
 340 more flexible in morphology), rendering them less than half the size of the PU 1000  
 341 equivalent. Cognate results were found for PU 500. Consequently, the average pore size for  
 342 the PU 1000 nanostructure was much larger than for the PU 2000 and PU 500 nanostructures,  
 343 with subsequent investigation evidencing its superior filtration performance. Further  
 344 optimization of the properties of the nanostructures could be facilitated by changing  
 345 the electrospinning conditions.



346

347 **Fig. 7.** Filtration performance of nanostructures with identical values for pressure drop, as  
 348 fabricated from PU with the inclusion of organic PPD soft segments; evaluation of their a)  
 349 filtration efficiency and b) quality factor.

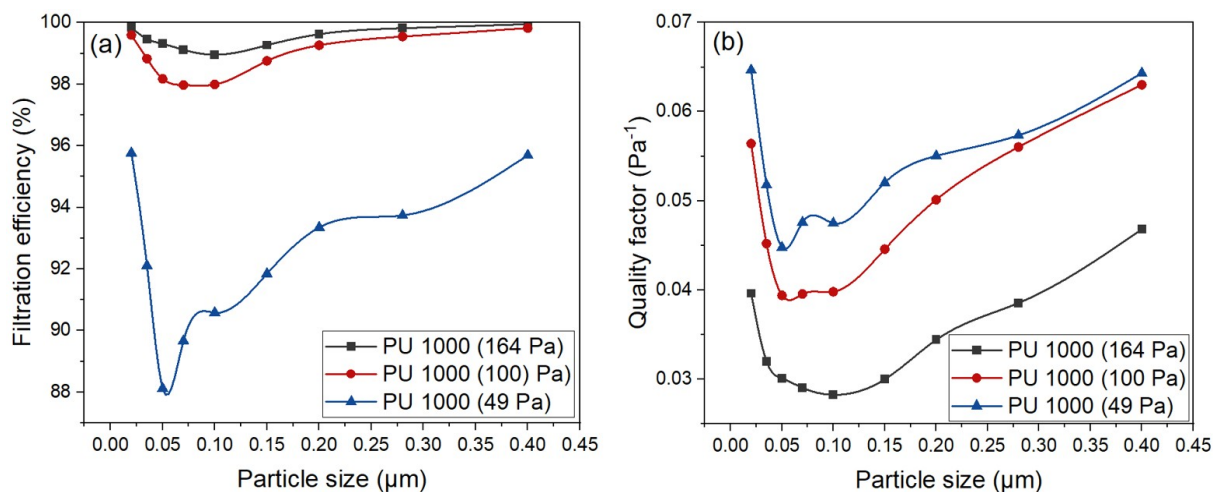
350 The significant differences in the pressure drops of the prepared filters complicated  
 351 the comparison of their filtration properties, requiring a contrast of calculated quality factors  
 352 instead (i.e. quality filters) to obtain such data [66]. The tendency for filtration presented  
 353 in Figure 7b was evidenced by evaluating this quality filter parameter at pressure drops  
 354 in excess of 100 Pa (Fig. 8b) and below 100 Pa (Fig. 8a). The best findings in this regard were  
 355 for materials with pressure drops of less than 100 Pa. Unfortunately, every filter fabricated  
 356 from PU 500 demonstrated values greater than that, as the fiber-forming process in the  
 357 electrostatic field was intense; thus, only the specimen with a minimal drop of 118 Pa is  
 358 included in Figure 8a.



359

360 **Fig. 8.** Quality factors for selected filters with pressure drops lower than 100 Pa (a) and higher  
 361 than 100 Pa (b).

362 The highest values for the aforementioned quality factor were obtained for filters derived  
 363 from PU synthesized with PPD 1000 soft segments at the molar ratio of MDI:PPD:BD =  
 364 4.7:1:3.7 (see Figs. 9a and 9b). Nanostructures at this ratio resulted in samples that had a  
 365 nanostructure morphology with a maximal pore size and the ability to capture ultra-fine  
 366 particles efficiently during Brownian motion. Filters showing values for the quality factor ( $q_F$ )  
 367 within the range of 30–70 kPa<sup>-1</sup> demonstrated superior filtration properties.



368

369 **Fig. 9.** Filtration efficiencies (a) and corresponding quality factors (b) for the best (PU 1000  
370 derived) filters.

371 Nanostructured layer (PU 1000) with high value of pore sizes (1.14 μm, Fig. 6b, Table 3),  
372 consequently low pressure drop (49 Pa, Fig. 8a) and high filtration efficiency in the area of  
373 ultrafine particles (Fig. 7a) are suitable with substantial benefit for combination with other  
374 microstructured air filtration materials (e.g. melt blown) for improvement of capture  
375 efficiency of SARS-CoV-2 virus incurring coronavirus disease.

## 376 CONCLUSION

377 This study focused on synthesizing bio-based PU that contained various arrangements of hard  
378 segment domains and lengths of soft segments. The resulting materials were evaluated via  
379 a series of physical-mechanical tests. Although varying the lengths of the soft segments  
380 and the structural arrangements of hard segments did not affect the hydrophilicity  
381 of the samples. It was discerned that thermal properties exerted a significant influence in this  
382 regard. With the growing length of the PPD soft segment in PU chains, the PU melting  
383 temperature is increasing and the glass transition temperature is decreasing. In spite of the fact  
384 that elastic moduli of synthesized PU were very similar in the range from 3520 to 3982 mPa s  
385 and fiber forming conditions in electrostatic field were the same, various nanostructures  
386 with distinct filtration properties were created, the effect of hard segment domains  
387 morphology and length of used soft segment being the reason. It proved impossible to judge  
388 separately the effects of fiber diameter and pore size on the filtration properties of  
389 nanostructured air filters fabricated to eliminate ultra-fine particles. The best filtration results  
390 were seen for materials prepared from PU with PPD soft segments at a molar weight of 1000  
391 g/mol. Prepared, more effective nanostructure has been formed by nanofibers with values of

392 fiber diameter  $218\pm 53$  nm and mean pore size  $1.14\pm 0.22$   $\mu\text{m}$ . Filters with pressure drops of 49  
393 Pa merely possessed a quality factor exceeding  $0.045$   $\text{Pa}^{-1}$ .

394

## 395 **ACKNOWLEDGEMENTS**

396 This work was supported from the European Just Transition Fund within the Operational  
397 Programme: Just Transition under the aegis of the Ministry of the Environment of the Czech  
398 Republic, project CirkArena number CZ.10.03.01/00/22\_003/0000045 and Operational  
399 Programme Johannes Amos Comenius OP JAC "Application potential development in the  
400 field of polymer materials in the context of circular economy compliance (POCEK)", number  
401 CZ.02.01.01/00/23\_021/0009004.

402 Authors are further grateful for co-funding from the development process of Centre of  
403 Polymer Systems, Tomas Bata University in Zlin, program DKRVO (RP/CPS/2024-28/002)  
404 supported by the Ministry of Education Youth and Sports of the Czech Republic. Muhammad  
405 Yasir also expresses his gratitude for support from the "Creativity, Intelligence & Talent for  
406 the Zlin Region" (CIT - ZK) programme. Simona Uhercová would also like to thank the  
407 Internal Grant Agency at Tomas Bata University in Zlin for its co-funding (project no.  
408 IGA/CPS/2024/003).

## 409 **CONFLICT OF INTERESTS**

410 The authors declare that no competing interests exist in connection with the research reported  
411 herein.

## 412 **REFERENCES**

- 413 [1] H. Sardon, D. Mecerreyes, A. Basterretxea, L. Avérous, C. Jehanno, From Lab to  
414 Market: Current Strategies for the Production of Biobased Polyols, *ACS Sustainable*  
415 *Chem. Eng.* 9 (2021) 10664–10677. <https://doi.org/10.1021/acssuschemeng.1c02361>.
- 416 [2] G. Woods, *The ICI Polyurethanes Book*, JOHN WILEY & SONS, New York, n.d.
- 417 [3] G. Rossignolo, G. Malucelli, A. Lorenzetti, Recycling of polyurethanes: where we are  
418 and where we are going, *Green Chem.* 26 (2024) 1132–1152.  
419 <https://doi.org/10.1039/D3GC02091F>.
- 420 [4] W. Ma, W. Cao, T. Lu, R. Xiong, C. Huang, Multifunctional nanofibrous membrane  
421 fabrication by a sacrifice template strategy for efficient emulsion oily wastewater  
422 separation and water purification, *Journal of Environmental Chemical Engineering* 10  
423 (2022) 108908. <https://doi.org/10.1016/j.jece.2022.108908>.
- 424 [5] C. Akduman, E.P.A. Kumbasar, Electrospun Polyurethane Nanofibers, in: F. Yilmaz  
425 (Ed.), *Aspects of Polyurethanes*, InTech, 2017.  
426 <https://doi.org/10.5772/intechopen.69937>.

- 427 [6] X. Pan, H. Wang, J. Wang, H. Wang, H. Shi, S. Wang, F. Ruan, Q. Feng, Composite  
428 Thermoplastic Polyurethane Nanofiber Membrane in Waterproof and Breathable  
429 Application, *Fibers Polym* 26 (2025) 2827–2837. <https://doi.org/10.1007/s12221-025-00986-1>.
- 431 [7] D. Kimmer, P. Slobodian, D. Petráš, M. Zatloukal, R. Olejník, P. Sába,  
432 Polyurethane/multiwalled carbon nanotube nanowebs prepared by an electrospinning  
433 process, *J of Applied Polymer Sci* 111 (2009) 2711–2714.  
434 <https://doi.org/10.1002/app.29238>.
- 435 [8] A. Shaker, A.T. Khedewy, M.A. Hassan, M.A.A. El-Baky, Thermo-mechanical  
436 characterization of electrospun polyurethane/carbon-nanotubes nanofibers: a  
437 comparative study, *Sci Rep* 13 (2023) 17368. <https://doi.org/10.1038/s41598-023-44020-x>.
- 439 [9] T. Debuissy, P. Sangwan, E. Pollet, L. Avérous, Study on the structure-properties  
440 relationship of biodegradable and biobased aliphatic copolyesters based on 1,3-  
441 propanediol, 1,4-butanediol, succinic and adipic acids, *Polymer* 122 (2017) 105–116.  
442 <https://doi.org/10.1016/j.polymer.2017.06.045>.
- 443 [10] J. Bozell, G. Petersen, Technology development for the production of biobased products  
444 from biorefinery carbohydrates—the US Department of Energy’s “Top 10” revisited,  
445 *Green Chemistry - GREEN CHEM* 12 (2010). <https://doi.org/10.1039/b922014c>.
- 446 [11] J. Becker, A. Lange, J. Fabarius, C. Wittmann, Top value platform chemicals: bio-based  
447 production of organic acids, *Current Opinion in Biotechnology* 36 (2015) 168–175.  
448 <https://doi.org/10.1016/j.copbio.2015.08.022>.
- 449 [12] I. Bechthold, K. Bretz, S. Kabasci, R. Kopitzky, A. Springer, Succinic Acid: A New  
450 Platform Chemical for Biobased Polymers from Renewable Resources, *Chemical  
451 Engineering & Technology* 31 (2008) 647–654. <https://doi.org/10.1002/ceat.200800063>.
- 452 [13] N.R. Barton, A.P. Burgard, M.J. Burk, J.S. Crater, R.E. Osterhout, P. Pharkya, B.A.  
453 Steer, J. Sun, J.D. Trawick, S.J. Van Dien, T.H. Yang, H. Yim, An integrated  
454 biotechnology platform for developing sustainable chemical processes, *J Ind Microbiol  
455 Biotechnol* 42 (2015) 349–360. <https://doi.org/10.1007/s10295-014-1541-1>.
- 456 [14] J.C. Khandaray, V.V. Gite, Fully biobased polyester polyols derived from renewable  
457 resources toward preparation of polyurethane and their application for coatings, *Journal  
458 of Applied Polymer Science* 136 (2019) 47558. <https://doi.org/10.1002/app.47558>.
- 459 [15] Synthesis of Biobased Polyurethane from Oleic and Ricinoleic Acids as the Renewable  
460 Resources via the AB-Type Self-Condensation Approach | *Biomacromolecules*, (n.d.).  
461 <https://pubs.acs.org/doi/10.1021/bm100233v> (accessed September 26, 2024).
- 462 [16] C. Zhang, S.A. Madbouly, M.R. Kessler, Biobased Polyurethanes Prepared from  
463 Different Vegetable Oils, *ACS Appl. Mater. Interfaces* 7 (2015) 1226–1233.  
464 <https://doi.org/10.1021/am5071333>.
- 465 [17] I. Bramhecha, J. Sheikh, Development of Sustainable Citric Acid-Based Polyol To  
466 Synthesize Waterborne Polyurethane for Antibacterial and Breathable Waterproof  
467 Coating of Cotton Fabric, *Ind. Eng. Chem. Res.* 58 (2019) 21252–21261.  
468 <https://doi.org/10.1021/acs.iecr.9b05195>.
- 469 [18] C. Zhang, S. Bhoyate, M. Ionescu, P.K. Kahol, R.K. Gupta, Highly flame retardant and  
470 bio-based rigid polyurethane foams derived from orange peel oil, *Polymer Engineering  
471 & Science* 58 (2018) 2078–2087. <https://doi.org/10.1002/pen.24819>.
- 472 [19] D. Kimmer, M. Kovarova, M. Yasir, L. Lovecka, J. Cisar, L. Musilova, J. Osicka, V.  
473 Sedlařík, Reinforced Fluorinated Copolymer and Polyurethane Electrospun Layered  
474 Nanofiber-Based Membranes for Effective Model Water Dead-End Microfiltration,  
475 *Polymers for Advanced Techs* 36 (2025) e70203. <https://doi.org/10.1002/pat.70203>.

- 476 [20] S. Gogoi, N. Karak, Biobased Biodegradable Waterborne Hyperbranched Polyurethane  
477 as an Ecofriendly Sustainable Material, *ACS Sustainable Chem. Eng.* 2 (2014) 2730–  
478 2738. <https://doi.org/10.1021/sc5006022>.
- 479 [21] L. Lovecká, M. Kovářová, D. Hanušová, D. Kimmer, A. Poláchová, V. Sedlařík,  
480 Application of green solvents as a replacement of toxic dimethylformamide in the  
481 polylactic acid electrospinning process, *Sustainable Materials and Technologies* 44  
482 (2025) e01405. <https://doi.org/10.1016/j.susmat.2025.e01405>.
- 483 [22] M. Ruan, H. Luan, G. Wang, M. Shen, Bio-polyols synthesized from bio-based 1,3-  
484 propanediol and applications on polyurethane reactive hot melt adhesives, *Industrial*  
485 *Crops and Products* 128 (2019) 436–444. <https://doi.org/10.1016/j.indcrop.2018.11.045>.
- 486 [23] M.A. Harmer, D.C. Confer, C.K. Hoffman, S.C. Jackson, A.Y. Liauw, A.R. Minter, E.R.  
487 Murphy, R.E. Spence, H.B. Sunkara, Renewably sourced polytrimethylene ether glycol  
488 by superacid catalyzed condensation of 1,3-propanediol, *Green Chem.* 12 (2010) 1410–  
489 1416. <https://doi.org/10.1039/C002443K>.
- 490 [24] C.E. McGlade, A review of the uncertainties in estimates of global oil resources, *Energy*  
491 47 (2012) 262–270. <https://doi.org/10.1016/j.energy.2012.07.048>.
- 492 [25] J.P.S. Aniceto, I. Portugal, C.M. Silva, Biomass-Based Polyols through Oxypropylation  
493 Reaction, *ChemSusChem* 5 (2012) 1358–1368. <https://doi.org/10.1002/cssc.201200032>.
- 494 [26] B. Ahvazi, O. Wojciechowicz, T.-M. Ton-That, J. Hawari, Preparation of Lignopolyols  
495 from Wheat Straw Soda Lignin, *J. Agric. Food Chem.* 59 (2011) 10505–10516.  
496 <https://doi.org/10.1021/jf202452m>.
- 497 [27] W. Chen, L. Zhong, X. Peng, R. Sun, F. Lu, Chemical Fixation of Carbon Dioxide Using  
498 a Green and Efficient Catalytic System Based on Sugarcane Bagasse—An Agricultural  
499 Waste, *ACS Sustainable Chem. Eng.* 3 (2015) 147–152.  
500 <https://doi.org/10.1021/sc5006445>.
- 501 [28] E.F. Gómez, X. Luo, C. Li, F.C. Michel, Y. Li, Biodegradability of crude glycerol-based  
502 polyurethane foams during composting, anaerobic digestion and soil incubation,  
503 *Polymer Degradation and Stability* 102 (2014) 195–203.  
504 <https://doi.org/10.1016/j.polymdegradstab.2014.01.008>.
- 505 [29] U.A. Amran, S. Zakaria, C.H. Chia, Z. Fang, M.Z. Masli, Production of Liquefied Oil  
506 Palm Empty Fruit Bunch Based Polyols via Microwave Heating, *Energy Fuels* 31 (2017)  
507 10975–10982. <https://doi.org/10.1021/acs.energyfuels.7b02098>.
- 508 [30] L. Hojabri, X. Kong, S.S. Narine, Fatty Acid-Derived Diisocyanate and Biobased  
509 Polyurethane Produced from Vegetable Oil: Synthesis, Polymerization, and  
510 Characterization, *Biomacromolecules* 10 (2009) 884–891.  
511 <https://doi.org/10.1021/bm801411w>.
- 512 [31] G. Lligadas, J.C. Ronda, M. Galià, V. Cádiz, Plant Oils as Platform Chemicals for  
513 Polyurethane Synthesis: Current State-of-the-Art, *Biomacromolecules* 11 (2010) 2825–  
514 2835. <https://doi.org/10.1021/bm100839x>.
- 515 [32] L. Serrano, M.G. Alriols, R. Briones, I. Mondragón, J. Labidi, Oxypropylation of  
516 Rapeseed Cake Residue Generated in the Biodiesel Production Process, *Ind. Eng. Chem.*  
517 *Res.* 49 (2010) 1526–1529. <https://doi.org/10.1021/ie9016732>.
- 518 [33] S. Desai, J. Patel, V. Sinha, Polyurethane adhesive system from biomaterial-based polyol  
519 for bonding wood, *International Journal of Adhesion and Adhesives* 23 (2003) 393–399.  
520 [https://doi.org/10.1016/S0143-7496\(03\)00070-8](https://doi.org/10.1016/S0143-7496(03)00070-8).
- 521 [34] A. Llevot, P.-K. Dannecker, M. von Czapiewski, L.C. Over, Z. Söyler, M.A.R. Meier,  
522 Renewability is not Enough: Recent Advances in the Sustainable Synthesis of Biomass-  
523 Derived Monomers and Polymers, *Chemistry – A European Journal* 22 (2016) 11510–  
524 11521. <https://doi.org/10.1002/chem.201602068>.

- 525 [35] H. Gang, D. Lee, K.-Y. Choi, H.-N. Kim, H. Ryu, D.-S. Lee, B.-G. Kim, Development  
526 of High Performance Polyurethane Elastomers Using Vanillin-Based Green Polyol  
527 Chain Extender Originating from Lignocellulosic Biomass, *ACS Sustainable Chem.*  
528 *Eng.* 5 (2017) 4582–4588. <https://doi.org/10.1021/acssuschemeng.6b02960>.
- 529 [36] O. Kreye, H. Mutlu, M.A.R. Meier, Sustainable routes to polyurethane precursors, *Green*  
530 *Chem.* 15 (2013) 1431–1455. <https://doi.org/10.1039/C3GC40440D>.
- 531 [37] H. Li, J.-T. Sun, C. Wang, S. Liu, D. Yuan, X. Zhou, J. Tan, L. Stubbs, C. He, High  
532 Modulus, Strength, and Toughness Polyurethane Elastomer Based on Unmodified  
533 Lignin, *ACS Sustainable Chem. Eng.* 5 (2017) 7942–7949.  
534 <https://doi.org/10.1021/acssuschemeng.7b01481>.
- 535 [38] W. Liu, T. Xie, R. Qiu, Biobased Thermosets Prepared from Rigid Isosorbide and  
536 Flexible Soybean Oil Derivatives, *ACS Sustainable Chem. Eng.* 5 (2017) 774–783.  
537 <https://doi.org/10.1021/acssuschemeng.6b02117>.
- 538 [39] D. Tang, B.A.J. Noordover, R.J. Sablong, C.E. Koning, Metal-free synthesis of novel  
539 biobased dihydroxyl-terminated aliphatic polyesters as building blocks for thermoplastic  
540 polyurethanes, *Journal of Polymer Science Part A: Polymer Chemistry* 49 (2011) 2959–  
541 2968. <https://doi.org/10.1002/pola.24732>.
- 542 [40] M. Burelo, I. Gaytán, H. Loza-Tavera, J.A. Cruz-Morales, D. Zárate-Saldaña, M.J. Cruz-  
543 Gómez, S. Gutiérrez, Synthesis, characterization and biodegradation studies of  
544 polyurethanes: Effect of unsaturation on biodegradability, *Chemosphere* 307 (2022)  
545 136136. <https://doi.org/10.1016/j.chemosphere.2022.136136>.
- 546 [41] K. Błazek, J. Datta, Renewable natural resources as green alternative substrates to obtain  
547 bio-based non-isocyanate polyurethanes-review, *Critical Reviews in Environmental*  
548 *Science and Technology* 49 (2019) 173–211.  
549 <https://doi.org/10.1080/10643389.2018.1537741>.
- 550 [42] Y. Ma, Y. Xiao, Y. Zhao, Y. Bei, L. Hu, Y. Zhou, P. Jia, Biomass based polyols and  
551 biomass based polyurethane materials as a route towards sustainability, *Reactive and*  
552 *Functional Polymers* 175 (2022) 105285.  
553 <https://doi.org/10.1016/j.reactfunctpolym.2022.105285>.
- 554 [43] D. Kimmer, M. Zatloukal, D. Petras, I. Vincent, P. Slobodian, Investigation of  
555 Polyurethane Electrospinning Process Efficiency, in: AIP Publishing LLC, Melville,  
556 New York, USA, 2009: pp. 305–311.
- 557 [44] R. Xu, J. Feng, L. Zhang, S. Li, Low viscosity of spinning liquid to prepare organic-  
558 inorganic hybrid ultrafine nanofiber membrane for high-efficiency filtration application,  
559 *Separation and Purification Technology* 303 (2022) 122224.  
560 <https://doi.org/10.1016/j.seppur.2022.122224>.
- 561 [45] H. Liu, Y. Zhu, C. Zhang, Y. Zhou, D.-G. Yu, Electrospun nanofiber as building blocks  
562 for high-performance air filter: A review, *Nano Today* 55 (2024) 102161.  
563 <https://doi.org/10.1016/j.nantod.2024.102161>.
- 564 [46] D. Kimmer, I. Vincent, L. Lovecka, T. Kazda, A. Giurg, O. Skorvan, Some aspects of  
565 applying nanostructured materials in air filtration, water filtration and electrical  
566 engineering, *AIP Conference Proceedings* 1843 (2017) 060001.  
567 <https://doi.org/10.1063/1.4983003>.
- 568 [47] T. Lu, J. Cui, Q. Qu, Y. Wang, J. Zhang, R. Xiong, W. Ma, C. Huang, Multistructured  
569 Electrospun Nanofibers for Air Filtration: A Review, *ACS Appl. Mater. Interfaces* 13  
570 (2021) 23293–23313. <https://doi.org/10.1021/acssami.1c06520>.
- 571 [48] D. Kimmer, I. Vincent, W. Sambaer, M. Zatloukal, J. Ondracek, Modeling and  
572 Preparation of Nanofibre and Composite Nanostructures, in: AIP Publishing LLC,  
573 Melville, New York, USA, 2015: pp. 050001-1-050001–6.  
574 <https://doi.org/10.1063/1.4918869>.

- 575 [49] W. Sambaer, M. Zatloukal, D. Kimmer, 3D air filtration modeling for nanofiber based  
576 filters in the ultrafine particle size range, *Chemical Engineering Science* 82 (2012) 299–  
577 311. <https://doi.org/10.1016/j.ces.2012.07.031>.
- 578 [50] D. Kimmer, I. Vincent, J. Fenyk, D. Petras, M. Zatloukal, W. Sambaer, V. Zdimal, M.  
579 Zatloukal, Morphology of Nano and Micro Fiber Structures in Ultrafine Particles  
580 Filtration, in: Zlin, (Czech Republic), 2011: pp. 295–311.  
581 <https://doi.org/10.1063/1.3604490>.
- 582 [51] W. Sambaer, M. Zatloukal, D. Kimmer, The use of novel digital image analysis  
583 technique and rheological tools to characterize nanofiber nonwovens, *Polymer Testing*  
584 29 (2010) 82–94. <https://doi.org/10.1016/j.polymertesting.2009.09.008>.
- 585 [52] Z. Sarac, A. Kilic, C. Tasdelen-Yucedag, Optimization of electro-blown polysulfone  
586 nanofiber mats for air filtration applications, *Polymer Engineering & Science* 63 (2023)  
587 723–737. <https://doi.org/10.1002/pen.26236>.
- 588 [53] W. Sambaer, M. Zatloukal, D. Kimmer, 3D modeling of filtration process via  
589 polyurethane nanofiber based nonwoven filters prepared by electrospinning process,  
590 *Chemical Engineering Science* 66 (2011) 613–623.  
591 <https://doi.org/10.1016/j.ces.2010.10.035>.
- 592 [54] T.T. Bui, M.K. Shin, S.Y. Jee, D.X. Long, J. Hong, M.-G. Kim, Ferroelectric PVDF  
593 nanofiber membrane for high-efficiency PM0.3 air filtration with low air flow resistance,  
594 *Colloids and Surfaces A: Physicochemical and Engineering Aspects* 640 (2022) 128418.  
595 <https://doi.org/10.1016/j.colsurfa.2022.128418>.
- 596 [55] C. Liu, P.-C. Hsu, H.-W. Lee, M. Ye, G. Zheng, N. Liu, W. Li, Y. Cui, Transparent air  
597 filter for high-efficiency PM2.5 capture, *Nat Commun* 6 (2015) 6205.  
598 <https://doi.org/10.1038/ncomms7205>.
- 599 [56] J.J. Huang, Y. Tian, R. Wang, M. Tian, Y. Liao, Fabrication of bead-on-string  
600 polyacrylonitrile nanofibrous air filters with superior filtration efficiency and ultralow  
601 pressure drop, *Separation and Purification Technology* 237 (2020) 116377.  
602 <https://doi.org/10.1016/j.seppur.2019.116377>.
- 603 [57] H. Wan, N. Wang, J. Yang, Y. Si, K. Chen, B. Ding, G. Sun, M. El-Newehy, S.S. Al-  
604 Deyab, J. Yu, Hierarchically structured polysulfone/titania fibrous membranes with  
605 enhanced air filtration performance, *Journal of Colloid and Interface Science* 417 (2014)  
606 18–26. <https://doi.org/10.1016/j.jcis.2013.11.009>.
- 607 [58] Y. Bian, S. Wang, L. Zhang, C. Chen, Influence of fiber diameter, filter thickness, and  
608 packing density on PM2.5 removal efficiency of electrospun nanofiber air filters for  
609 indoor applications, *Building and Environment* 170 (2020) 106628.  
610 <https://doi.org/10.1016/j.buildenv.2019.106628>.
- 611 [59] B. Liu, S. Zhang, X. Wang, J. Yu, B. Ding, Efficient and reusable polyamide-56  
612 nanofiber/nets membrane with bimodal structures for air filtration, *Journal of Colloid  
613 and Interface Science* 457 (2015) 203–211. <https://doi.org/10.1016/j.jcis.2015.07.019>.
- 614 [60] D. Kowalczyk, M. Pitucha, Application of FTIR Method for the Assessment of  
615 Immobilization of Active Substances in the Matrix of Biomedical Materials, *Materials*  
616 12 (2019) 2972. <https://doi.org/10.3390/ma12182972>.
- 617 [61] I.D. dos Santos Silva, A. Albuquerque, L. Boskamp, A. Ries, K. Haag, K. Koschek, R.  
618 Wellen, Synthesis of bio-polyurethanes with isosorbide and propanediol based  
619 poly(lactic acid) diol, *Journal of Applied Polymer Science* 140 (2023) e53623.  
620 <https://doi.org/10.1002/app.53623>.
- 621 [62] B. Quienne, N. Kasmi, R. Dieden, S. Caillol, Y. Habibi, Isocyanate-Free Fully Biobased  
622 Star Polyester-Urethanes: Synthesis and Thermal Properties, *Biomacromolecules* 21  
623 (2020) 1943–1951. <https://doi.org/10.1021/acs.biomac.0c00156>.

- 624 [63] P. Somdee, T. Lassú-Kuknyó, C. Kónya, T. Szabó, K. Marossy, Thermal analysis of  
625 polyurethane elastomers matrix with different chain extender contents for thermal  
626 conductive application, *J Therm Anal Calorim* 138 (2019) 1003–1010.  
627 <https://doi.org/10.1007/s10973-019-08183-y>.
- 628 [64] B. Pukánszky Jr., K. Bagdi, Z. Tóvölgyi, J. Varga, L. Botz, S. Hudak, T. Dóczy, B.  
629 Pukánszky, Effect of Interactions, Molecular and Phase Structure on the Properties of  
630 Polyurethane Elastomers, in: Z.D. Hórvölgyi, É. Kiss (Eds.), *Colloids for Nano- and*  
631 *Biotechnology*, Springer Berlin Heidelberg, Berlin, Heidelberg, 2008: pp. 218–224.  
632 [https://doi.org/10.1007/2882\\_2008\\_102](https://doi.org/10.1007/2882_2008_102).
- 633 [65] M. Abiad, M. Carvajal, O. Campanella, A Review on Methods and Theories to Describe  
634 the Glass Transition Phenomenon: Applications in Food and Pharmaceutical Products,  
635 *Food Engineering Reviews* 1 (2009) 105–132. [https://doi.org/10.1007/s12393-009-9009-](https://doi.org/10.1007/s12393-009-9009-1)  
636 1.
- 637 [66] W.C. Hinds, *Aerosol Technology, Properties, Behavior, and Measurement of Airborne*  
638 *Particles*, 2nd ed., JOHN WILEY & SONS, New York, n.d.
- 639